

Air oxidation and molten salt corrosion studies on bimetallic boiler steel at elevated temperatures

Appala Naidu A^a, Kumaresh Babu S.P^a, Manikandan M^{b*}, Arivarasu M^b,

Devendranath Ramkumar K^b, Arivazhagan N^b

^aDepartment of Metallurgical and Materials Engineering, National Institute Of
Technology, Triuchirapalli –620115, India

^bSchool Of Mechanical and Building Science, Vellore Institute Of Technology,
Vellore–632014, India

*Corresponding author: mano.manikandan@gmail.com

Abstract

Understanding the behavior of bimetallic joint at elevated temperatures and especially their corrosion behavior has become an object of scientific investigation recently. This paper reports on the high temperature corrosion behavior of bimetallic joint of SA-387 Gr 22 and SA-387Gr11 in air and molten salt environment of (Na₂SO₄–48% NaCl) at 650 °C and 800 °C under cyclic condition. The influence of molten salt on hot corrosion and oxidation has been discussed in detail. The corrosion kinetics of specimens with and without molten salt deposits indicated a parabolic growth of oxides. The resulting oxide scale in the weldment has been characterized systematically using surface

analytical technique such as XRD and SEM/EDS analysis to evaluate the possible mechanisms of corrosion compounds are discussed.

Keywords: air oxidation, molten salt, hot corrosion kinetics, boiler steel, power plant environment.

1. Introduction

Hot corrosion of bimetallic joints is a serious problem in power generating equipment, air craft, industrial waste incinerators, paper and pulp industries, petro chemical industries, metallurgical furnaces, IC engines and in other energy conversion systems. Fossil-fuel boilers experience hot corrosion problems in the components of steam generators, water walls surrounding the furnace, economizer assemblies, and in the front and rear portion of the super heaters and re-heaters [1–3]. Welding is an inevitable joining method for power generating equipment, where combination of similar and dissimilar joints exists. Carbon steels and Cr–Mo steels find wide applications in power plant equipments. Corrosion aspects of these materials made by FCAW still require a vast amount of research and development. The combinations of such an elevated temperature with an environment that contains contaminants such as sodium sulfate, sodium chlorides and various halides require special attention to the

phenomenon of hot corrosion. These forms of hot corrosion consume the material at a very rapid rate [4].

Hurdus et.al. [1] noticed that fine grained structure results in an increase in the active reaction, quicker formation of protective and self healing scales, more sites for oxide nucleation as well as the scales at the grain boundaries and within the grains.

Singh Raman et.al. and wyatt [5–7] have noticed that the steel with high silicon and coarse grain showed the best resistance to high temperature corrosion. The external surface of the super heater tubes is covered with a thick layer of metal oxide mainly iron oxide (Fe_3O_4) formed by oxidation in the presence of excess oxygen. This layer may be converted in to iron sulfate by reaction with molten alkali metal sulfate. The sulfate has low melting points, in the range of 250 °C–400 °C and may react as acidic molten salt with iron oxides and with metallic iron. The formation of various carbides and intermetallic phases has been reported to degrade the weldment property [8–10]. The rate of precipitation of M_{23}C_6 carbide and intermetallics are faster in the weld metal than in the wrought material.

The present investigation is aimed to evaluate the behavior of bimetallic joint of SA–387Gr22 and SA–387 Gr11 at two different temperatures at 650 °C and 800 °C exposed in air oxidation as well as molten salt power plant environment of (Na_2SO_4 – 48%NaCl).

The corrosion products were characterized using the combined techniques of X-ray diffraction (XRD), and scanning electron microscopy (SEM/EDS).

2. Experimental Details

2.1. Hot Corrosion test

Bimetallic joint employing SA387 Gr22 and SA387 Gr11 was taken up in this study and their chemical compositions are shown in Table. 1.

Corrosion test has been carried out in air as well as molten salt environment. Specimens for hot corrosion tests are fabricated using FCA welding process. To facilitate the hot corrosion tests, the samples ($20 \times 5 \times 10$ mm) were cut in the weld zone, heat affected zone, and base metal by wire cut electrical discharge machining (EDM). Mirror polishing down to $1 \mu\text{m}$ by alumina on a cloth polishing wheel is carried out before the corrosion run. Immediately, a coating of uniform thickness with $3\text{--}5 \text{ mg/cm}^2$ of salt mixture was applied with a camel hair brush on the preheated sample (250°C). On these specimens, cyclic studies were performed in the air as well as molten salt ($\text{Na}_2\text{SO}_4\text{--}48\%\text{NaCl}$) for exactly 50 cycles at two different temperatures (650°C and 800°C). The duration of each cycle is for 1 h 20 mins in which heating is for one hour at $650 / 800^\circ\text{C}$ in a silicon carbide tube furnace followed by 20 mins of cooling at room temperature. During the corrosion tests, the weight change measurements were

taken at the end of each cycle using an electronic weighing balance machine which has a sensitivity of 1 mg. The spalled scale was also retained during the measurement of the weight change to determine the total rate of corrosion. Efforts were made to formulate the kinetics of corrosion and the same is presented in this paper. The samples after corrosion tests are subjected to characterization studies using SEM/EDS and XRD for surface analysis of the scale.

3. Results and Discussion

3.1. Corrosion kinetics

The corrosion kinetics of specimens with and without molten salt deposits is depicted in (Fig 1– 4) as a plot of weight gain per unit area vs. function of time (number of cycles). These figures indicate that the weight gain kinetics under air oxidation shows a steady-state parabolic rate law, whereas the molten salt environment is a multi stage weight-gain growth rate. It is observed from the graph that all the specimens follow nearly parabolic rate law.

3.2. X-Ray Diffraction Analysis.

XRD analysis has been studied on the specimen after exposed to air oxidation and molten salt environment after corrosion cycle and is shown in Fig 5–6. It is evident that

the hot corroded weldments have Fe_2O_3 as the main phase along with relatively weak

peaks of Cr_2O_3 , Fe_3O_4 and MnO were indicated. With increase in the temperature of corrosion studies, the higher content of Cr_2O_3 , Fe_2O_3 in scale over the interface is observed, which may be due to enrichment of this zone with Fe and Cr with continuous inter-diffusion of elements during hot corrosion cycles. According to Arivazhagan et al. [11], in the molten salt environment, the resistance to corrosion for all the steels is less than that in air. Thus has been ascribed to the presence of sodium and sulfur which accelerates the corrosion of steels. Furthermore spalling may be one of the reasons for enhanced corrosion.

3.3. SEM/EDAX analysis

SEM/EDS result of the scale formed on the coupon after 50 cycles of oxidation in air at 650 and 800 °C represented in Fig 7–8. The superior corrosion rate shown by weld zone might be the formation of irregular porous scale consists oxides of Fe and Cr acts as a oxygen carrier. Simultaneously, the pores scale is destroyed or eliminated by oxidation and consequently the metal surface is exposed to direct action of aggressive environment as has been indicated in the current investigation. Further, the fine crystal of scale in the HAZ near to weld zone consists of higher amount of oxides (Cr and Fe) at 800 °C.

environment by keeping 650 °C and 800 °C is shown in Fig 9–10. EDAX analysis for the samples after air oxidation as well as molten salt environment shows Fe_2O_3 to be the predominant phase in the entire region. However Cr_2O_3 content is higher in the scale of weld zone. Moreover some minor constituent of MoO_3 and MnO were observed on the weldment as seen. The EDS results witnessed that the hot corrosion in molten salt shown that extensive corrosion can take place at higher temperatures due to change in salt chemistry [12–13] and/or sulfur penetration through scales [14–15]. Generally, a fluxing mechanism was proposed for explaining hot corrosion behavior of alloys. According to this model, the reaction of a metal with Na_2SO_4 and the removal of sulfur from the melt resulted in high melt basicity, or the reaction of refractory metal oxides with the salt resulted in high melt acidity. The oxide formed on the alloy surface could dissolve in to the molten salt. The eutectic point of (Na_2SO_4 – 48% NaCl) salt is 618 °C. Therefore, the salt molten during corrosion tests at 650 °C and 800 °C sodium sulphate may dissociate according to the following reactions.



Based on lewis acid–base concept, in reaction (1) Na_2O was basic component, and SO_3

was acidic component. SO_3 is in equilibrium with S_2 and O_2 as shown in reaction (2).

Therefore, when the oxygen partial pressure decreases, the sulfur partial pressure will increase. This mechanism will result in the increasing of sulfur partial pressure in the molten salt, when the oxygen is consumed

The Cl_2 produced is able to penetrate through oxide scales quickly along cracks or pores and then react with oxide and Ni, Al and other elements in the super alloy. Some volatile chlorides such as AlCl_3 and NiCl_2 would be formed [16–17]. The volatile chlorides may diffuse outward through the cracks or pores to the outer surface. At the surface of the scales, where the oxygen potential is high, the chlorides may re-oxidize. The Cl_2 , except that which evaporated outward, reacted cyclically with Al, Ni and other elements in the super alloy, which increased the corrosion rate.

4. Conclusions

1. Thermo–gravimetric analysis showed that the weld and weld interface have more prone to corroded as compared to the base metal in both air and molten salt environment.
2. The effect of temperature showed the significant effect on the bimetal joint corrosion resistance in both air as well as molten salt environment.

3. The air oxidation showed the lowest weight gain as compared in case of molten salt ($\text{Na}_2\text{SO}_4 - 48\%\text{NaCl}$) environment.
4. SEM/EDS and XRD analysis has indicated the presence of Fe_2O_3 as a predominant phase in the molten salt environment and Fe_2O_3 , Fe_3O_4 a predominant phase in the oxidation.
5. The corrosion kinetics shows the parabolic behavior in both air and molten salt power plant environment.

REFERENCES

- [1] 'Observation of oscillating reaction rates during the isothermal oxidation of ferritic steels', M.H. Hurdus, L. Tomlinson, J.M. Tichmarsh, *Oxid. Met.*, 34, 5–6, 429–464, 1990.
- [2] 'Corrosion in power generating equipment', G.J. Theus and P.L. Daniel, *Proceedings of the Eighth International Brown Boveri Symposium*, Baden, Switzerland, 185, 1983.
- [3] 'Corrosion estimating of chemical cleaning solvents', NACE, NACE Publication, *Material Performance*, 182, 1982,.
- [4] 'Hot corrosion in gas turbine components', N. Eliaz, G. Shemesh, R.M. Latanision, *Eng. Fail. Anal.*, 9, 31–43, 2002.

- [5] 'Influence of prior-austenite grain size on the oxidation behavior of 9 wt.% Cr-1 wt.% Mo steel', R.K. Singh Raman and J.B. Gnanamoorthy, *Oxid. Met.*, 38, 5-6, 483-496, 1992.
- [6] 'Oxidation behavior of 2.25Cr-1Mo steel with prior tempering at different temperatures', R.Singh, R.K. Raman, J.B. Gnanamoorthy, S.K. Roy, *Oxid. Met.*, 40, 1-2, 21-36, 1993.
- [7] 'The performance of Cr-Mo steels in the boilers of CEGB power stations', Wyatt, *Proceedings of the International Conference on Ferritic Steels For Fast Reactor Steam Generators*, 27, 2, 1978.
- [8] 'Mechanical properties of stainless steel weld metal at elevated temperature with special regard to the influence of ferrite', S. Polgari, ESAB Technical Report No. SDA 83001, 1982.
- [9] 'Microstructure-property correlation of thermally aged type 316L stainless steel weld metal', T.P.S. Gill, M. Vijayalakshmi, P. Rodriguez, K.A. Padmanabhan, *Metal Trans.*, 20, 6, 1115-1124, 1989.
- [10] 'Creep Fracture at stress concentrations in type 316 stainless steel weld metal', G.J. Lloyd, E. Barker, R. Pilkington, *Mater Sci Eng.*, 74, 2, 159-177, 1985.
- [11] 'Hot Corrosion Behavior of Friction Welded AISI 4140 and AISI 304 in K₂SO₄-60% NaCl Mixture', N. Arivazhagan, K. Senthilkumaran, S. Narayanan, K.D.

28, 10,895–904, 2012.

- [12] ‘Deposition – Hot Corrosion In Gas Turbine Engines’, N.S. Bornstein and M.A. Decrescent, ASME, 81 –GT-153, 4p, 1981.
- [13] ‘Simultaneous sulfidation–oxidation of nickel at 603°C in argon–so₂ atmospheres’, K.L. Luthra, and W.L. Worrell, metallurgical Transactions A, 9, 8,1055–1061, 1978.
- [14] ‘The high–temperature oxidation of nickel–20 wt. % chromium alloys containing dispersed oxide phase’, J. Stringer, B.A. Wilcox, R.I. Jaffee, Oxid. Met., 5, 1, 11–47, 1972.
- [15] S. Taniguchi, and T. Shibata, Transactions of the Japan Institute of Metals, 29, 658, 1988.
- [16] ‘Proc. symp. on High Temperature Alloys for Gas Turbines, Riedel’, B. Jianting, D. Ranuci, E. Picco, P.M. Strocchi, Dordrecht, P.805, 1982.
- [17] ‘High Temperature Alloy Corrosion By Halogens’, P. Elliot, C.J. Tyreman, R. Prescott, Journal of Metals, 37, 20-23, 1985.

Legends for Figures

Figure 1 Thermo gravimetric graph for air oxidised SA-387Gr22 and SA-387Gr11

bimetallic joint at 650 °C

- Figure 2 Thermo gravimetric graph for air oxidised SA-387Gr22 and SA-387Gr11 bimetallic joint at 800 °C
- Figure 3 Thermo gravimetric graph for hot corroded SA-387Gr22 and SA-387Gr11 bimetallic joint in molten salt at 650 °C
- Figure 4 Thermo gravimetric graph for hot corroded SA-387Gr22 and SA-387Gr11 bimetallic joint in molten salt at 800 °C
- Figure 5 X-ray Diffraction patterns for corroded bimetallic joint for SA-381-Gr22 & Gr22 WM, SA-381-Gr22 BM and Gr11 HAZ boiler steels subjected to cyclic Oxidation at 800 °C and 650 °C for 50 cycles.
- Figure 6 X-ray diffraction patterns for corroded bimetallic joint in SA-381-Gr11, SA-381-Gr22 boiler steels subjected to cyclic Hot Corrosion at 800 °C for 50 cycles.
- Figure 7 SEM/EDS results of GR11 and GR22 bimetallic joint after exposed in air oxidation at 650°C
- Figure 8 SEM/EDS results of GR11 and GR22 bimetallic joint after exposed in air oxidation at 800°C
- Figure 9 SEM/EDS results of GR11 and GR22 bimetallic joint after exposed in molten salt at 650 °C
- Figure 10 SEM/EDS results of GR11 and GR22 bimetallic joint after exposed in molten salt at 800 °C

Legends for the table

Table 1 Chemical composition of Base metal and Filler wire.

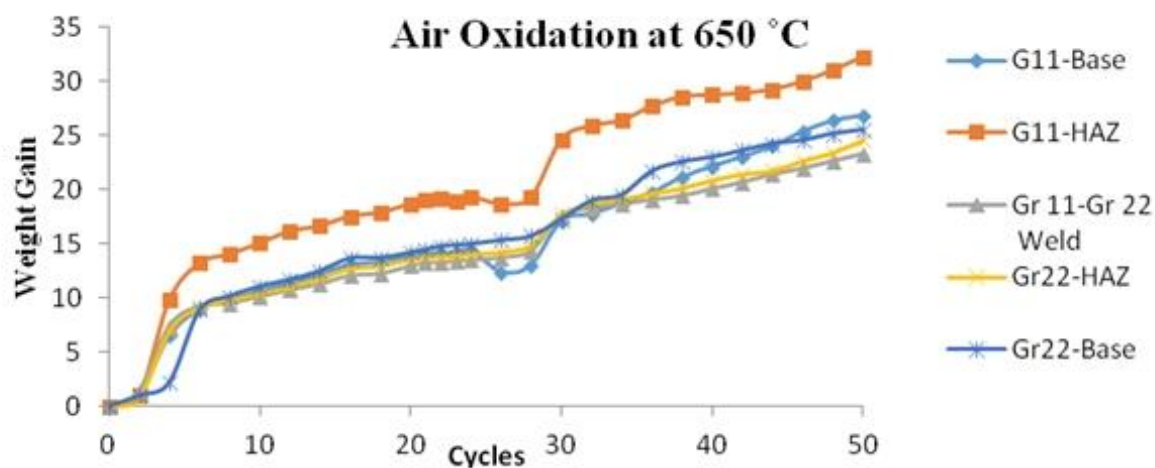


Figure 1

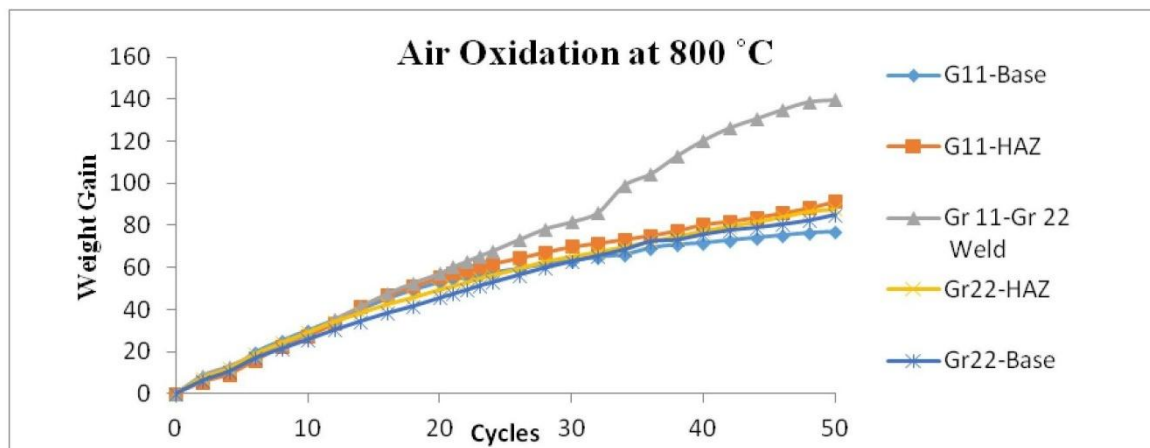


Figure 2

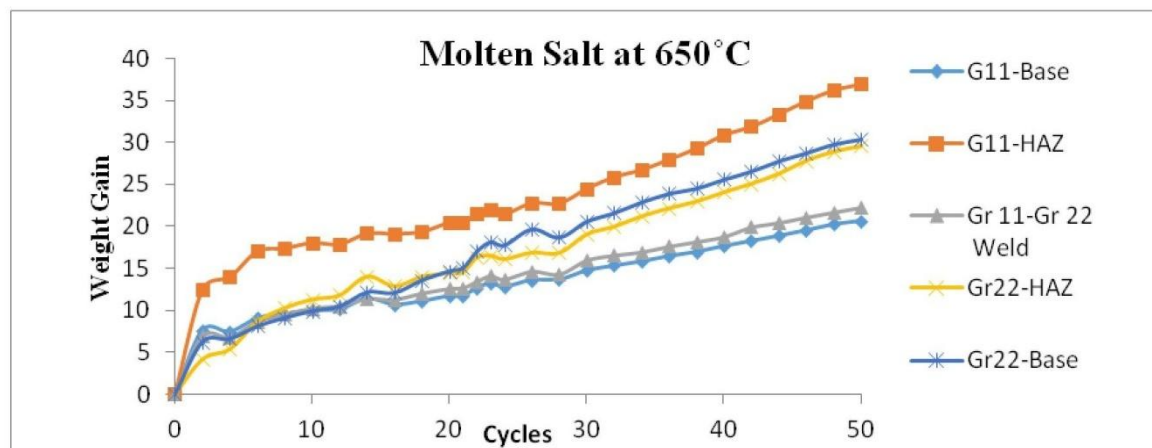


Figure 3

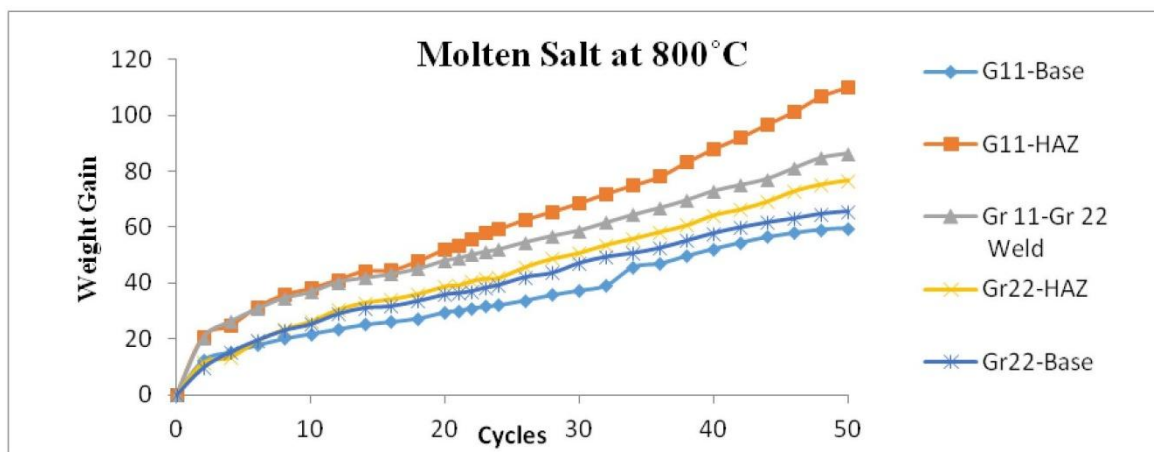


Figure 4

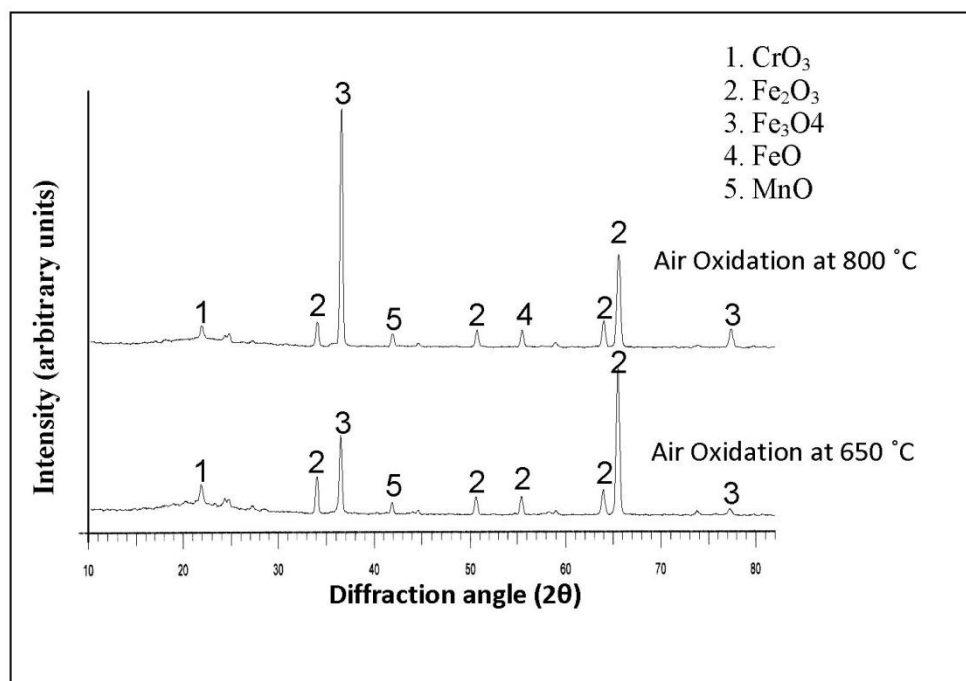


Figure 5

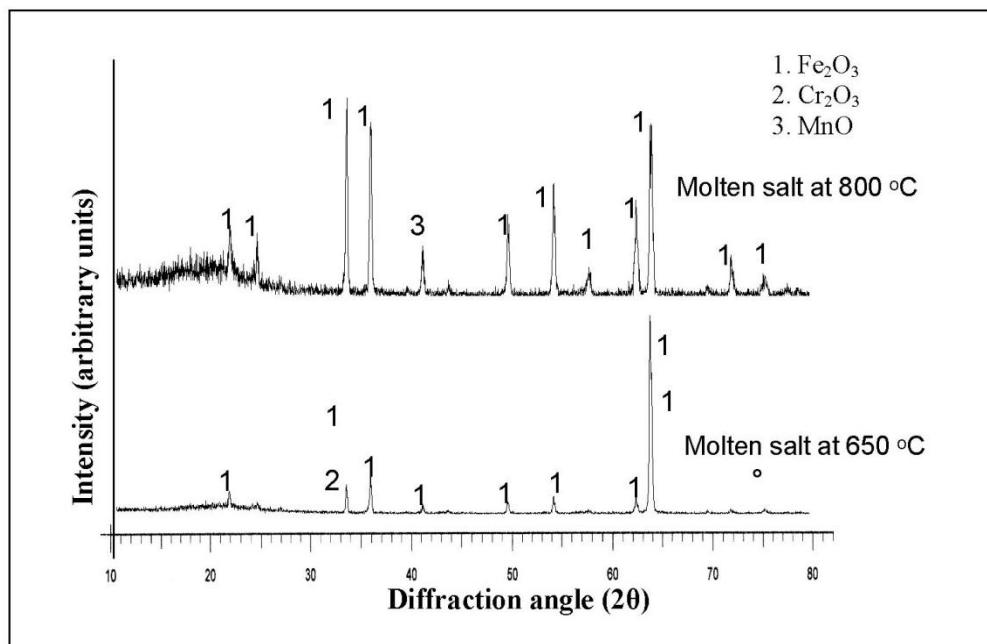


Figure 6

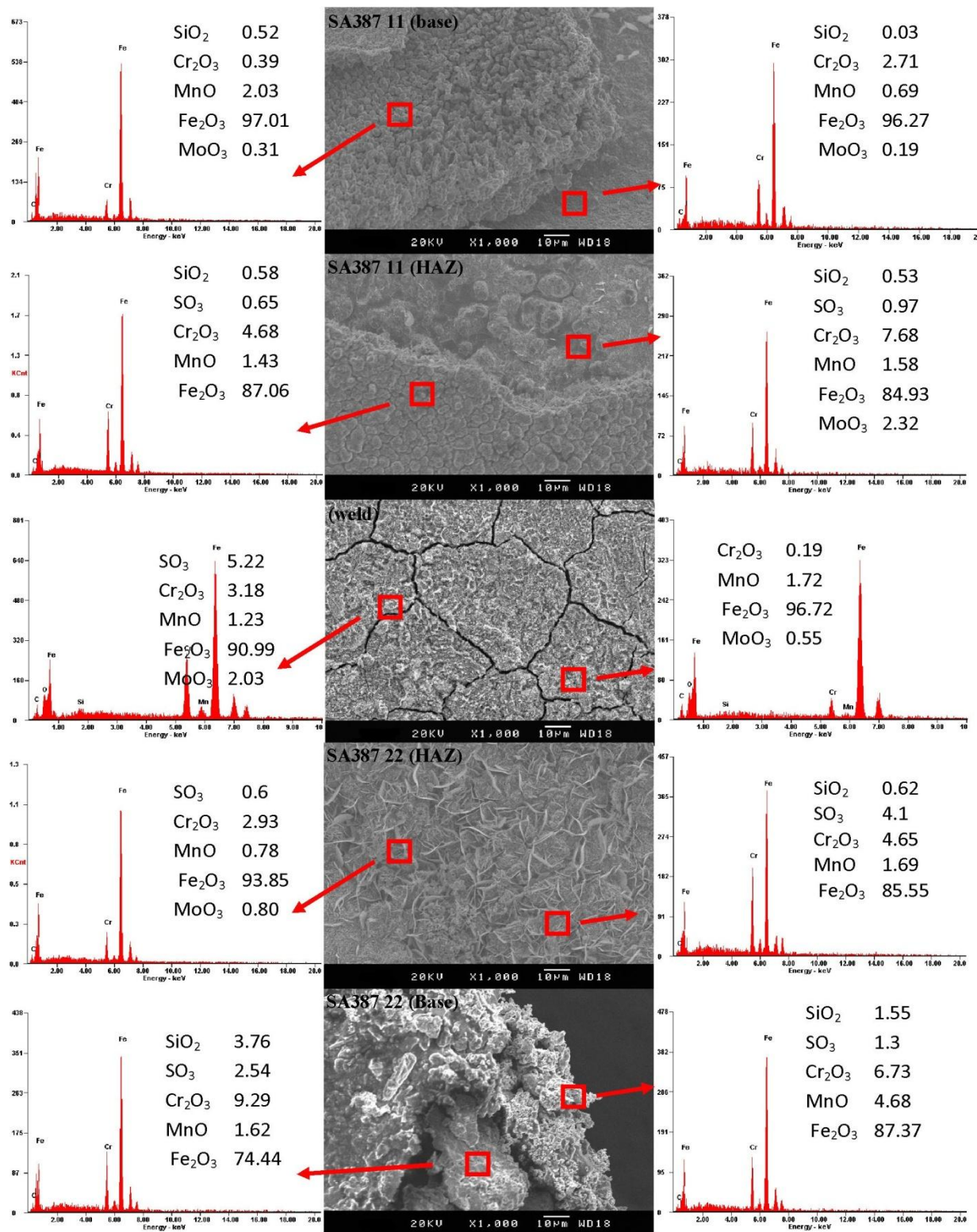


Figure 7

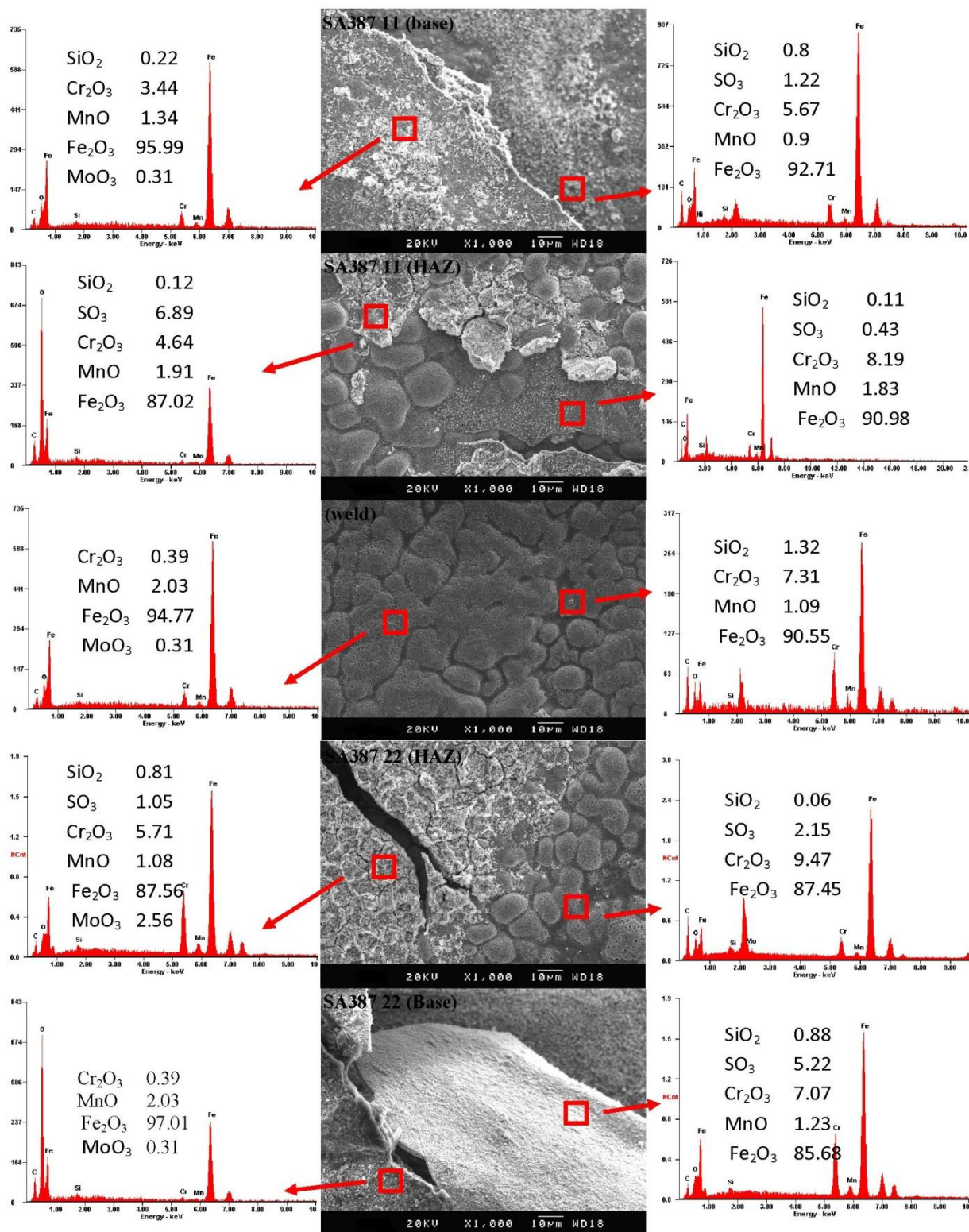


Figure 8

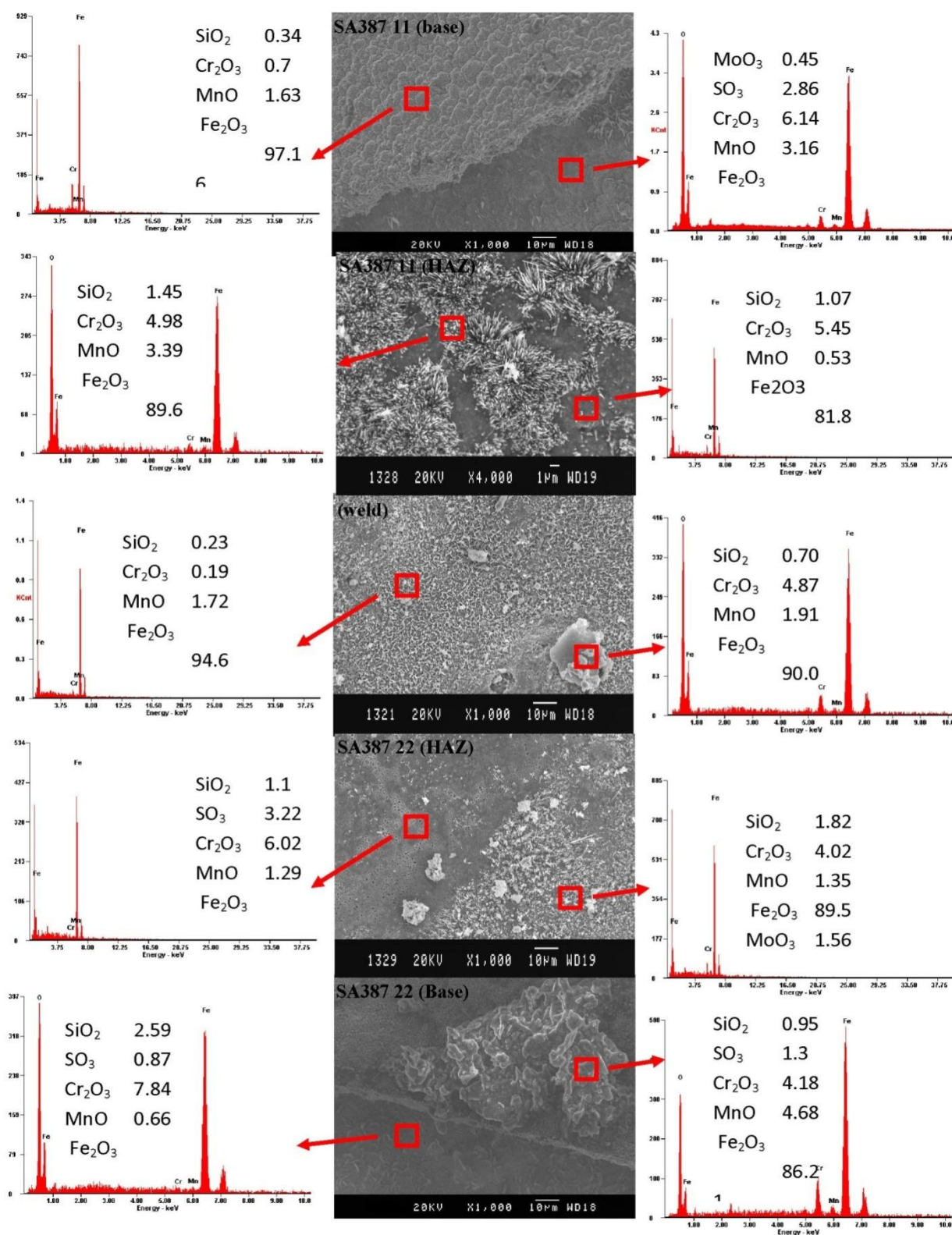


Figure 9

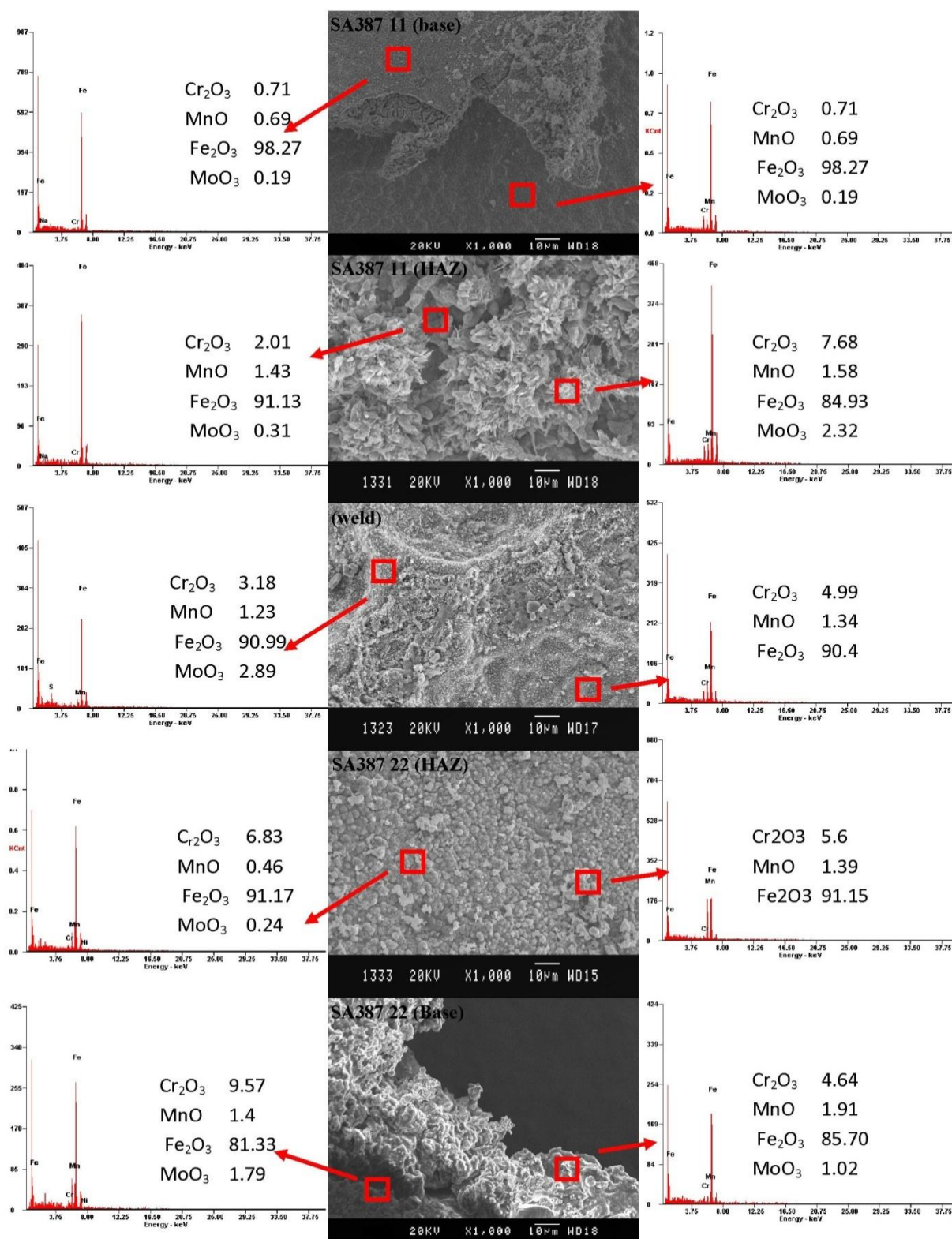


Figure 10

Table 1 Chemical composition of base metal and filler wire.

Element	C	Mn	Si	P	S	Mo	Cr	Ni	Cu	Fe
SA-387Gr11	0.15 max	0.3- 0.6	0.5- 1.0	0.03 max	0.03 max	0.45- 0.65	1.0-1.5	-	-	Bal.
SA-387Gr22	0.15 max	0.3- 0.6	0.5- 1.0	0.03 max	0.03 max	0.9-1.2	2-2.5	-	-	Bal.
E90T5-B3	0.12 max	1.5 max	0.60 max	0.025	0.025	1.10 max	2.5 max	0.20	0.30	Bal